Development of a Cell-Based Fluorescence Polarization Biosensor Using Preproinsulin to Identify Compounds That Alter Insulin Granule Dynamics

Na Young Yi,[1] Qingping He,[1] Thomas B. Caligan,[1] Ginger R. Smith,[1] Lawrence J. Forsberg,[2] Jay E. Brenman,[2] and Jonathan Z. Sexton[1]

[1]Biomanufacturing Research Institute and Technology Enterprise, Department of Pharmaceutical Sciences, North Carolina Central University, Durham, North Carolina.
[2]The Neuroscience Center and Department of Cell Biology & Physiology, UNC Chapel Hill School of Medicine, Chapel Hill, North Carolina.

ABSTRACT

Diabetes currently affects 9.3% of the U.S. population totaling $245 billion annually in U.S. direct and indirect healthcare costs. Current therapies for diabetes are limited in their ability to control blood glucose and/or enhance insulin sensitivity. Therefore, innovative and efficacious therapies for diabetes are urgently needed. Herein we describe a fluorescent insulin reporter system (preproinsulin-mCherry, PPI-mCherry) that tracks live-cell insulin dynamics and secretion in pancreatic β-cells with utility for high-content assessment of real-time insulin dynamics. Additionally, we report a new modality for sensing insulin granule packaging in conventional high-throughput screening (HTS), using a hybrid cell-based fluorescence polarization (FP)/internal FRET biosensor using the PPI-mCherry reporter system. We observed that bafilomycin, a vacuolar H^+ ATPase inhibitor and inhibitor of insulin granule formation, significantly increased mCherry FP in INS-1 cells with PPI-mCherry. Partial least squares regression analysis demonstrated that an increase of FP by bafilomycin is significantly correlated with a decrease in granularity of PPI-mCherry signal in the cells. The increased FP by bafilomycin is due to inhibition of self-Förster resonant energy transfer (homo-FRET) caused by the increased mCherry intermolecular distance. FP substantially decreases when insulin is tightly packaged in the granules, and the homo-FRET decreases when insulin granule packaging is inhibited, resulting in increased FP. We performed pilot HTS of 1782 FDA-approved small molecules and natural products from Prestwick and Enzo chemical libraries resulting in an overall Z′-factor of 0.52 ± 0.03, indicating the suitability of this biosensor for HTS. This novel biosensor enables live-cell assessment of protein–protein interaction/protein aggregation in live cells and is compatible with conventional FP plate readers.

INTRODUCTION

Reduced insulin secretion or increased insulin resistance leads to serious metabolic disturbances that characterize diabetes mellitus.[1] Diabetes affects ~10% of the U.S. population totaling $245 billion annually in total medical costs.[2] Injectable insulin is a well-known therapy for type-1 (insulin-dependent) diabetes. However, most diabetes is type-2 diabetes (T2D) associated with obesity, Western diet, and sedentary lifestyle. In fact T2D represents greater than 90% of all diabetes cases in the United States.[3] In addition, T2D diabetes incidence also increases with age—23% of individuals over age 60 have diabetes[4]—and aging populations will create increased diabetes costs in the future. Clearly, given the escalating magnitude of T2D costs and complications, therapeutic innovation for T2D treatment remain of high interest and importance.

Need for New Antidiabetics

Measurement of glycated hemoglobin (HbA1c [or A1c]) is used as a surrogate index of past blood glucose levels to diagnose and subsequently monitor/treat diabetes. Currently the diagnosis of diabetes is confirmed when HbA1c rises above 6.5%.[5] The large market size for T2D drugs and need for better glycemic (A1c) control or better tolerated drugs create a constant search for new treatments.

The main pharmacological approaches for treating early stage (noninsulin-dependent) T2D are by (1) alleviating insulin resistance in peripheral tissues thereby making endogenous insulin more effective with insulin sensitizers; (2) stimulating additional endogenous insulin secretion in the pancreas with secretagogues; and (3) increasing glucose uptake by peripheral tissues, including fat. The first-line antidiabetes drug, generic

DOI: 10.1089/adt.2015.665

metformin, acts primarily by decreasing glucose output from the liver, but has side effects (gastrointestinal events and lactic acidosis)[6] and does not always maintain sufficient glycemic control over time.[7] First-line treatment typically starts with diet/exercise modification progressing to oral monotherapy (typically metformin) to combination oral therapy to exogenous insulin.[8] Despite numerous classes of T2D drugs, only ~36% of diabetes patients achieve the A1c goal of ≤7%.[9] In addition, some diabetes drugs (*e.g.*, thiazolidinediones) actually lead to weight gain, an undesirable side effect and itself a risk factor for diabetes.

New classes of drugs that normalize blood glucose by stimulating glucose-dependent insulin secretion (*i.e.*, post-meal) are the insulin incretins. The incretins act through the glucagon-like peptide-1 receptor (GLP-1R), which is the receptor for the gut hormone glucagon-like peptide-1 (GLP-1). Much of the recent pursuit of antidiabetic drug development has focused on GLP-1R or the enzyme that degrades it, DPP-4 (dipeptidyl peptidase-4)[10]; however, to date, there has not been clinical success in molecularly targeting GLP-1R with small orally available molecule agonists.

The mechanism of action of GLP-1 is unique in that it induces glucose-dependent stimulation of insulin secretion while suppressing glucagon production. Compounds that cause glucose-dependent insulin secretion are highly attractive because when blood glucose levels are in the normal fasting range, GLP-1 does not stimulate insulin secretion, rather only when blood glucose levels rise. These agents generally do not cause hypoglycemia as do the legacy insulin secretagogues, including the sulfonylureas (SFUs—glyburide, glipizide, and glimepiride) and the glinides (repaglinide and nateglinide), which have substantial side effects, including acute hypoglycemia and weight gain. The major downside to current FDA-approved incretin mimetics includes peptide administration through subcutaneous injection. Although the GLP-1 receptor has so far been refractory to small molecule drug development, other molecules in the pathway or different pathways in the cell that might elicit similar biological responses may be amenable to small molecule agonism/antagonism.

Insulin Cell Biology as an Assay Development Target

The ability to secrete physiologically active insulin is regulated at multiple steps, each providing the opportunity for pharmacological intervention (*Fig. 1*). Insulin production begins with regulated transcription and subsequent translation of the preproinsulin (PPI) peptide. PPI is sequentially formed by a signal peptide, the B chain, the C peptide, and the A chain. Proteolytic cleavage of the signal peptide forms proinsulin. Subsequent removal of C peptide from proinsulin

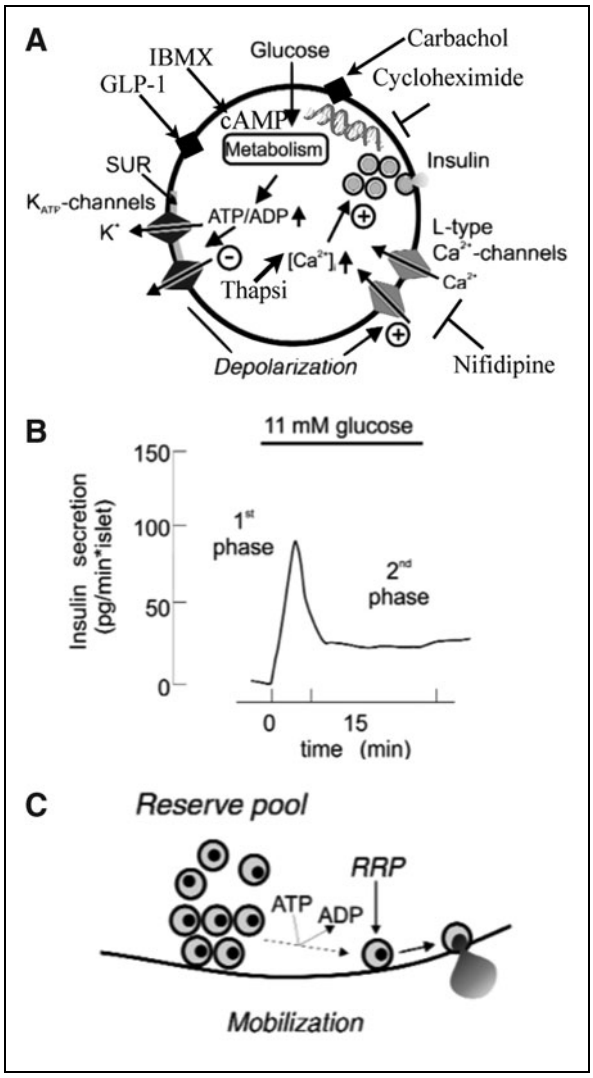

Fig. 1. Insulin secretion mechanisms described in pancreatic beta cells (adapted from Rorsman[1]). **(A)** Secretion signaling elements of the β-cell: SUR-sulfonylurea receptor, ATP-regulated K^+ channel, Ca^{2+} channel, and mechanistic tool compounds. **(B)** Biphasic insulin response to glucose, and **(C)** insulin secretion from readily releasable pool (RRP) and ATP-dependent replenishment by the reserve pool (RP).

produces active mature insulin. Several key cell biological events must occur for insulin maturation: (1) transcription, (2) translation and translocation in the endoplasmic reticulum, (3) folding, oxidation (disulfide bonding between peptide chains), and signal peptide cleavage, (4) Golgi transport, vesicle packaging into secretory vesicles, and (5) protease/carboxypeptidase cleavage to produce mature insulin. Insulin maturation also requires acidification of secretory vesicles to a pH typically near 5.0. Once mature insulin is formed, it is stored inside the cell as dense-core granules in two distinct populations; (1) the readily releasable pool (RRP) for

immediate response to stimulus, and (2) the reserve pool for replenishment of the RRP (*Fig. 1C*).[11]

The physiological response to glucose is a two-stage (biphasic) release response consisting of a sharp rise, followed by a gradual second phase release (*Fig. 1B*). The first phase of insulin release requires a rapid rise in intracellular Ca^{2+} and corresponds to the immediate release of insulin granules from the RRP. These mature insulin vesicles sit near the membrane waiting for an appropriate stimulus to trigger membrane fusion and release. A portion of the remaining granules (reserve pool) are mobilized to replenish the RRP and sustain insulin secretion.[1] Pharmacological agents that directly modulate insulin secretion target various steps in the insulin synthesis and secretion pathways. Complex signaling networks from ion channels (potassium and voltage-dependent Ca^{2+} channels) to G protein–coupled receptors regulate insulin secretion. Known tool compounds that alter insulin synthesis/maturation and secretion are shown in *Figure 1A*.

Homo-FRET and Fluorescence Polarization in HTS

When fluorescent molecules are excited by plane-polarized light, the emitted light retains the polarization of the excitation source due to selective absorption of photons by molecules where the absorption dipole moment is aligned with the polarization of the incident photon. The observed fluorescence anisotropy is decreased when molecular rotation happens in solution during the lifetime of the excited state. Rotation of the transition dipole along with the molecule will correspondingly rotate the polarization of the emitted photon. Additionally, increasing molecular size (hydrodynamic radius) slows the tumbling rate of the fluorophore and slows the observed depolarization of emission. The fluorescence polarization (FP) phenomenon has been widely used to assay binding events in biochemical systems because the tumbling rate of a fluorophore can change dramatically upon binding events (*e.g.*, small molecule dye binding to a larger protein).

When a single fluorophore is in sufficiently high concentration, Förster resonance energy transfer (FRET) can occur between fluorophores of the same type, called homo-FRET.[12,13] In the homo-FRET interaction, an excited state hops nonradiatively from one fluorescent molecule to another through a dipole–dipole interaction. When there is a substantially high local concentration of a fluorophore or the intermolecular distance is below 10 nm, homo-FRET can occur. When excitation occurs with plane-polarized light and homo-FRET occurs, the energy transfer from one fluorophore to the next causes a relative decrease in the FP signal due to randomization of the transition dipole through successive charge transfer events.[14] We reasoned we could exploit the high-density packaging of insulin granules to utilize homo-FRET. Homo-FRET can be used to assess protein dynamics in live cells by monitoring the FP anisotropy using a conventional FP plate reader. In this study, we exploit homo-FRET through FP (HF-FP) to assess the dynamics of insulin granule packaging using a genetically encoded mCherry-fusion with the insulin B and C peptide that colocalizes with endogenous insulin granules.

HTS and Screening for Insulin-Modulating Compounds

Numerous high-throughput screening (HTS) campaigns have been performed in the diabetes therapeutic area directed at both discrete molecular and phenotypic targets thought to modulate some aspect of insulin production and release. In recent years, compounds that stimulate the incretin effect—glucose-dependent insulin secretion—have been of particular interest to pharmaceutical companies. Insulin granule packaging is a critical upstream step in the insulin release cascade; however, the factors or compounds that affect insulin granule packaging have not been widely investigated and insulin granule packaging remains inaccessible in HTS. Agents that influence insulin biosynthesis may alter insulin granule packaging by increasing or decreasing insulin synthesis at the level of gene transcription, translation, or posttranslational modification. Also, compounds that affect insulin secretion may modify insulin granule packaging. Inhibitors of insulin release, such as mitochondrial toxins, may cause mature insulin granules to be more tightly packaged and factors that increase insulin secretion may lead to a lesser amount of packaged insulin. Therefore, a simple plate-reader-based assay to monitor insulin packaging will provide an invaluable tool for investigating potential insulin-modulating compounds and also represents a valid phenotypic target for enhancing insulin production/processing.

MATERIALS AND METHODS

PPI mCherry Reporter Constructs

Previous studies using a green fluorescent protein (GFP) fusion to the C peptide of mouse PPI II produced localization with and release of endogenous insulin.[15] We have utilized this approach toward labeling endogenous insulin through fluorescently tagged PPI. Additionally, we have replaced the GFP moiety with the much less pH-sensitive mCherry to prevent loss of fluorescent signal during vesicle maturation, as insulin vesicles undergo acidification to as low as pH 4.5 during maturation. We have also included the 3′-UTR region of the PPI mRNA as this has been shown to confer a glucose-induced increase in mRNA stability.[16,17] Our constructs were packaged in a pLenti delivery system, and the reporter signal was driven by either

© MARY ANN LIEBERT, INC.

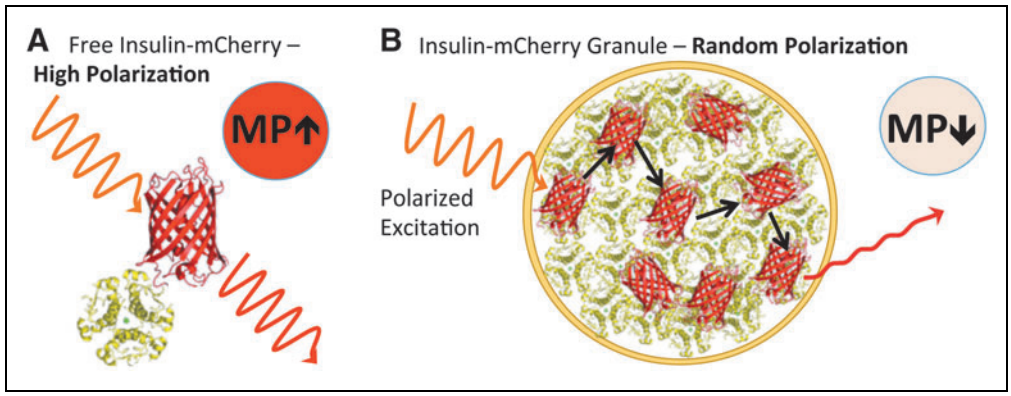

Fig. 2. Schematic of homo-FRET detection through fluorescence polarization (FP) for the sensitive monitoring of insulin granule packaging in live cells with insulin shown in *yellow* and mCherry shown in *red*. **(A)** Free insulin-mCherry with polarized excitation and emission with conserved polarization. **(B)** Mixed mCherry-insulin and endogenous insulin within a dense core granule. Plane polarized excitation of mCherry and subsequent hopping of the excited state, leading to emission with randomized polarization. MP indicates that relative millipolarization units are high for **(A)** and low for **(B)**.

cytomegalovirus (CMV) or mouse insulin promoter. All constructs were made using pLenti X2 Puro Empty (w609-1; Addgene). To produce mCherry with an insulin-targeting sequence at its N-terminus driven by a CMV promoter, we cloned the portion of mouse insulin II upstream of GFP from the Adlox-InC-emGFP construct (a gift from Dr. Peter Drain),[15] including the signal peptide, B chain, and the C peptide up to Pro72, inserting into the *EcoR*I and *BamH*I sites of pmCherry-N1 (*Fig. 2A*).

Cell Culture, Transfection, and Flow Cytometry

Rat insulinoma (INS-1) cells were cultured in RPMI-1640 medium (Sigma -Aldrich) with 10% fetal bovine serum (FBS), 2 mM glutamine, 1 mM sodium pyruvate, 10 mM HEPES, 0.05 mM 2-mercaptoethanol, and 1% penicillin and streptomycin. The cells were grown at 37°C with 5% CO_2 in fully humidified air. For transfection, INS-1 cells were transfected with our reporter construct driven by CMV promoter using Lipofectamine 2000 (Invitrogen). Two days following the transfection, cells were selected with 350 μg/mL of G418 until colonies were visible. After the antibiotic selection, the transfected INS-1 cells were subjected to FACS sorting to pool cells according to mCherry fluorescence intensity (low, medium, and high), and the cells that highly expressed mCherry fluorescence were used for our experiments.

Human Islet Cell Culture, Viral Transduction, and Flow Cytometry

Human pancreatic islets were obtained from the National Disease Research Interchange (NDRI) or Prodo lab. Body mass index of the donors was within the normal range. The purity and viability of islets ranged from 85% to 95%. Handling of human islets was carried out according to legal provisions and rules of the North Carolina Central University. However, review of the Institutional Review Board was exempt. The islets were dispersed into a single cell suspension by brief digestion with trypsin and allowed to attach and recover overnight. The following day, islets were transduced with lentivirus particles. The lentivirus particles were generated in HEK293 cells using the PPI-mCherry reporter being expressed under control of mouse PPI II promotor. Following 3 days of viral transduction, the maximum fluorescent signal intensity was observed and flow cytometry was performed to isolate mCherry-positive cells. Sorted, mCherry-positive cells were stained with Hoechst-33342 and YoYo-1 iodide and high-content imaging was performed using a BD pathway 855 microscope (Becton Dickenson) to determine viability and yield of β-cells.

Immunofluorescence

Cells were grown on poly-D-lysine (50 μg/mL)-coated BD Falcon culture slides and were fixed with 4% paraformaldehyde (Fisher Scientific) and washed with phosphate-buffered saline (PBS) three times. Cells were permeabilized for 10 min in PBS containing 0.2% Triton X-100 in PBS (TPBS) and blocked with 5% bovine serum albumin (BSA) in TPBS buffer for 1 h. Cells were incubated with primary guinea pig anti-insulin antibody (1:100; Dako) or mouse anti-glucagon antibody (Abcam) diluted in TPBS containing 1% BSA overnight at 4°C. Cells were then washed and incubated for 1 h with secondary AlexaFluor 488-conjugated secondary antibody (1:500; Life Technology). Images were taken using both a Nikon confocal microscope (Nikon Eclipse-C) and a BD pathway 855 microscope.

Glucose-Stimulated Insulin Secretion

The parental INS-1 cells and the transfected cells were seeded at a density of 5×10^5 cells/well in six-well plates in complete growth medium and were grown to 90% confluence. The cells were washed with PBS and maintained for 2 h in glucose-free Dulbecco's modified Eagle's medium (DMEM). The cells were then incubated for 1 h at 37°C in 2 mL of DMEM containing low glucose (5.6 mM), high glucose (25 mM) alone,

and high glucose (25 mM) in the presence of 10 nM Exendin-4 (Cat. No. 1933; TOCRIS Bioscience) or 10 μM nifedipine (Cat. No 151743; MP Biomedicals, LLC). Following incubation, supernatants were collected to determine secreted insulin contents.

Quantification of Secreted Insulin

Following glucose-stimulated insulin secretion (GSIS), 800 μL of harvested cultured medium and human insulin standard were directly deposited onto nitrocellulose membrane using a minifold-1 dot-blot system (Whatman, Inc.), and the membrane was scanned using the 680 nm channel on an Odyssey imaging system (Li-Cor Biosciences) to detect mCherry signal (excitation 560/40 nm and emission 630/75 nm). In addition, the membranes were blocked for 1 h then probed with guinea pig anti-insulin (1:5,000; Dako) followed with secondary antibody (LI-COR IRDye 800 donkey anti-guinea pig at 1:5,000 dilution). The dot-blot was scanned and quantified with the Odyssey infrared imaging system.

Tracking of Insulin Transport in Live Cells (Live Cell Imaging)

Transfected INS-1 cells were seeded onto a 96-well poly-D-lysine-coated imaging plate (BD Bioscience) and were grown to 70% confluence. Following 2 h incubation in glucose-free DMEM, the medium was replaced with DMEM containing 25 mM glucose with 10 nM Exendin-4. Plates were immediately imaged with a BD pathway 855 microscope, and automated image analysis was performed using Cell Profiler® software to quantitate mCherry intensity and granularity/textural features.

Bafilomycin as a Positive Control for HF-FP Assay Development

Transfected INS-1 cells were plated on a 96-well poly-D-lysine-coated, NUNC black/clear bottom tissue culture-treated imaging plates at cell density of 1.0×10^5 cell/well and incubated for 2 days until 95% confluence was reached. To determine the effective concentration and incubation time of bafilomycin for HF-FP assay development, cells were incubated in a medium containing bafilomycin (12.5–200 nM) for 1, 2, 4, or 6 h. The entire volume of media (200 μL) was removed and 150 μL of media was added by hand using a multichannel pipette. Immediately after media change, FP was measured using a PHERAstar microplate reader (BMG LABTECH) with the FP module (excitation, 590-50 nm; emission, 675-50 nm; focal height, 4.8; Flashes per well, 200/well; cycle time, 300 ms/well). FP values were expressed in millipolarization (mP) units and the mP values were calculated using the equation $mP = 1{,}000\times(I_{\parallel}-I_{\perp})/(I_{\parallel}+I_{\perp})$, where $I_{\parallel}$ is the parallel emission intensity and $I_{\perp}$ is the perpendicular emission intensity measurements. Automatic gain adjustment was optimized to achieve a target mP value of 400 and gain settings were fixed for the duration of screening.*

High-Content and PLS Regression Analysis

Transfected INS-1 cells were seeded at a density of 5×10^5 on 96-well NCNC plate and cultured for 2 days. Then, cells were treated with 0.1–200 nM of bafilomycin for 4 h and FP was measured. Following FP, cells were fixed with 4% formaldehyde and stained with 10 μg/mL Hoechst-33342. The cells were then washed once with PBS and imaged on a BD Pathway 855 BioImager using a 20×/0.75 NA Olympus UPlanApo objective lens. Images were analyzed using CellProfiler software[18] and mCherry features were tabulated from cells, including granularity, texture, and average mCherry intensity. Granularity was calculated within CellProfiler using the MeasureGranularity module. Partial least squares (PLS) regression was performed using JMP11 software (SAS) for exploratory data analysis to find linear combinations of cellular features from high-content analysis that were highly correlated with the measured FP result to aid in understanding insulin granule phenotypes with respect to the measured FP signal.

Pilot Screening in 384-Well Format

To validate HF-FP for HTS using laboratory automation, pilot screening was performed in the 384-well format. The assay protocol is presented in *Table 1*. Two highly annotated small-molecule libraries were used, including a 1,280-molecule FDA-approved drug set (Prestwick Chemical Library) and 502 purified natural products (Enzo Life Sciences). The compound libraries were plated in Axygen 384-well rigid PCR plates (Cat. No. 321-67-051) in 100% DMSO at 5 mM for single concentration screening.

Transfected INS-1 cells were plated in 384-well poly-D-lysine-coated, NUNC black/clear bottom tissue culture-treated imaging plates (NUNC No. 152029). Twenty-five microliters of prewarmed growth medium was added to each well using a Mutidrop-384 (Thermo/Fisher), followed by 25 μL of cell suspension (80,000 viable cells/well). The cells were cultured for 48 h at 37°C with 5% CO_2. Forty microliters of growth medium was removed and 50 μL of fresh medium was added with a BioMek NX using 96-well head with AP96 P20 tips. A Pintool array (V&P Scientific) was used for compound

*mP values are arbitrary and highly dependent on detector gain, however, mP values for controls were similar day to day.

© MARY ANN LIEBERT, INC.

Table 1. Protocol for HF-FP High-Content Assay

Step	Parameter	Value	Description
1	Plate cells	25 + 25 μL	80,000 PPI-mCherry INS-1 cells/well
2	Cell attachment	48 h	37°C, 5% CO_2
3	Media change		Removed 40 μL and added 50 μL of media
4	Add vehicle	50 nL	DMSO control added to columns 1 and 2
5	Add bafilomycin	50 nL	Bafilomycin added to columns 23 and 24 at final concentration of 83 nM
6	Add library compounds	50 nL	Compounds added to columns 3–22 at final concentration of 4.2 μM
7	Incubation	4 h	37°C, 5% CO_2
8	Media change		Removed 40 μL and added 50 μL of media
9	Assay readout	Excitation at 590 nm, emission at 675 nm	PHERAstar microplate reader

Step Notes

1. Plated in 384-well NUNC poly-D-lysine-coated, black/clear bottom tissue culture-treated plates.
3. The Biomek NX with 96-well head was used to remove and add media.
4. DMSO controls were used for minimum signal of homo-FRET FP.
5. Bafilomycin-treated wells were used for maximum signal of HF-FP.
6. Prestwick Chemical Library and Enzo Life Sciences natural product library were tested. Pintool was used to transfer the compounds into the assay plates. Final DMSO concentration was 0.1%.
8. The Biomek NX with 96-well head was used to remove and add media.
9. Plates were read from the top.

FP, fluorescence polarization; FRET, Förster resonance energy transfer.

addition for an ~1,000-fold dilution. Fifty nanoliters of 5 mM compound in DMSO was added to columns 3–22 of the plate for single-concentration screening. Fifty nanoliters of DMSO and 100 μM of bafilomycin were added to negative control wells in columns 1 and 2 and positive control wells in column 23 and 24, respectively. Following 4 h of incubation with compounds, media were changed by Biomek NX workstation, and then FP was measured using a PHERAstar microplate reader (excitation, 590-50 nm; emission, 675-50 nm; focal height, 7.2; Flashes per well, 200/well; cycle time, 300 ms/well). Compounds were identified as hits if the mP values were above or below the 95% CL (approximately $\mu \pm 3\sigma$) for the samples in the plate. Instant JChem was used for structure database management, search and prediction (Instant JChem 15.1.12, 2015; ChemAxon [http://www.chemaxon.com]).

EC_{50} dose–response determination was performed in triplicates in a 384-well plate. Compounds selected from the pilot screen were diluted in a 10-point twofold format using an HP D300 digital dispenser (HP) that directly dispenses compounds to each well of the cell plate, thereby avoiding a serial dilution step. Two microliters of selected hits and bafilomycin (100 μM) were added to each reservoir. The controls were applied to column 1–2 (DMSO—minimum signal control) and 23–24 (83 nM of bafilomycin—maximum signal control), and different concentrations of the test compounds were applied to column 3–22 of the cell plate. The concentrations ranged from 16.67 to 0.03 μM for Prestwick compounds, and 8.33 to 0.02 μM for the Natural product compounds. The final DMSO concentration was normalized to 0.2% by the HP D300.

RESULTS

We have developed a genetically encoded insulin reporter system based on a PPI peptide-mCherry fluorescent protein fusion to enable tracking of insulin dynamics in live cells using both high-throughput and high-content screening, sorting of β-cells, and for rapid determination of GSIS by detecting secreted mCherry fluorescence. Initial studies have focused on utilization and validation of the insulin reporter system for HTS to detect compounds that significantly alter insulin granule packaging. To achieve this goal, we have developed a unique modality for HTS using FP anisotropy to detect changes in the packaging of mCherry in living cells through homo-FRET.

Figure 2A shows a schematic of normal fluorescence anisotropy for the PPI-mCherry protein. Upon excitation with plane-polarized light, the fluorescence emission exhibits high polarization anisotropy. *Figure 2B* shows a schematic of homo-FRET between mCherry molecules inside a dense-core insulin granule. The plane-polarized excitation is absorbed and the excited state hops from molecule to molecule by FRET, thereby reducing the polarization anisotropy.

Validation and Utility of the PPI-mCherry Biosensor

We established a reporter construct consisting of mCherry fused with PPI under CMV promoter control (*Fig. 3A*) that fluorescently labels endogenous insulin granules. *Figure 3B* shows transfected INS-1 cells with PPI-mCherry reporter and *Figure 3C* demonstrates excellent colocalization between immunostained endogenous insulin and PPI-mCherry in transfected INS-1 cells. To establish the utility in primary human cells, human pancreatic islets were virally transduced with the PPI-mCherry reporter construct (driven by the mouse insulin

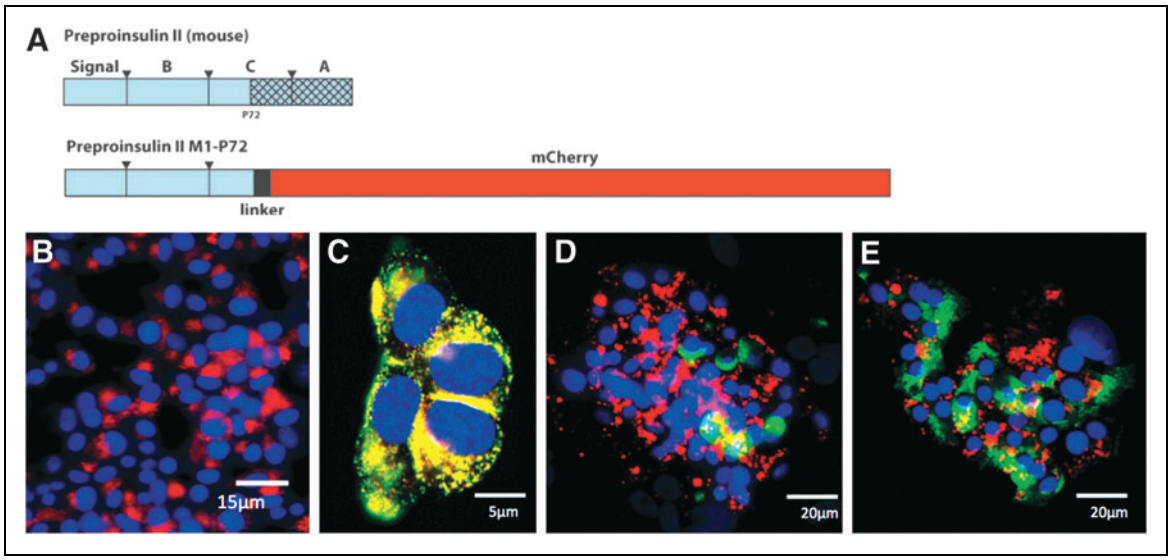

Fig. 3. PPI-mCherry reporter system. **(A)** Schematic diagram of PPI-mCherry reporter construct. A part of C-peptide and entire A chain of mouse preproinsulin (PPI) II were replaced with mCherry. **(B)** Immunofluorescent image of transfected INS-1 cells with PPI-mCherry reporter. **(C)** Colocalization of PPI-mCherry with insulin in INS-1 cells. The *yellow/orange color* indicated a high extent of colocalization of PPI-mCherry (*red*) and insulin vesicles (*green*) in the INS-1 cells. In the human islets, glucagon (*green*) was not colocalized with the mCherry reporter. **(D)** The extent of colocalization of PPI-mCherry reporter and insulin (*green*) was not significant **(E)**. (nuclei = *blue*).

promoter). The transduced islets show discrete β-cell labeling when the islets are costained for glucagon (*Fig. 3D*). However, a partial colocalization was observed between PPI-mCherry and immunostained endogenous insulin in the transduced islets (*Fig. 3E*).

We have also observed that the PPI-mCherry protein is secreted through normal insulin secretory channels and can be directly detected by measuring mCherry fluorescence secreted into the media. GSIS was performed using the PPI-mCherry INS-1 cell line and we observed an approximate two-fold glucose-stimulated release of the PPI-mCherry reporter in high glucose media compared with no glucose media (*Fig. 4A*). The parental INS-1 cells have historically shown a two- to three-fold GSIS over baseline.[15] The addition of exendin-4 (10 nM) displayed a synergistic response with high glucose (2.7-fold compared to low glucose). This response was inhibited by the calcium channel blocker nifedipine that is known to inhibit insulin release.[19] These data suggest that PPI-mCherry reporter system: (1) undergoes GSIS and does not interfere with secretion of endogenous insulin and, (2) responds normally to known insulin-modulating compounds, such as exendin-4 and nifedipine in similar quantitative fashion as insulin.

Labeling of primary human islets was performed with lentiviral transduction of the PPI-mCherry reporter system and proof-of-principal of β-cell sorting was performed. *Figure 4B* shows adequate separation for sorting in the mCherry channel. Following sorting, mCherry-positive cells were seeded

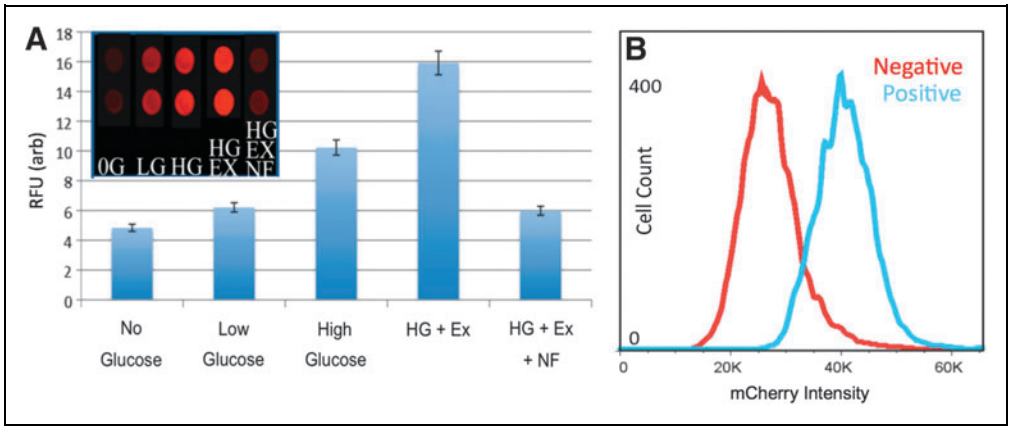

Fig. 4. Validation and utilization of the biosensor using a fluorescent PPI reporter. **(A)** Glucose and exendin-4 stimulated insulin secretion. *Inset* shows relative fluorescent intensity of secreted mCherry-insulin. **(B)** Flow cytometry histogram for primary human β-cell sorting. LG, low glucose (5.6 mM); HG, high glucose (25 mM); Ex, exendin-4 10 nM; NF, nifedipine 10 μM; RFU, relative fluorescence units.

© MARY ANN LIEBERT, INC.

onto 384-well plate (2,000/well) and automated microscopy was performed to capture three-color multiplexed images for each well; nuclei (blue—Hoechst-33342—cell permeant nucleic acid stain), viability (green—YoYo-1 iodide, cell impermeant nucleic acid stain), and insulin (red—PPI-mCherry). Image analysis is subsequently performed to tabulate the number of cells/well, live:dead score based on the percentage of YoYo-1-positive cells, and β-cell confirmation by mCherry. Post sorted β-cells were found to be highly viable after 3 days in culture (>95%), and the mCherry-positive β-cells comprised over 85%. The maximum theoretical yield for β-cells from dispersed islets is ∼70%. We obtained ∼50% yield from a small batch of 250,000 dispersed cells yielding ∼140,000 β-cells.

Live cell kinetic imaging was performed using our reporter system to visualize intracellular insulin vesicle movement, and localization (*e.g.*, readily releasable vs. reserve pools). Immediately after adding high glucose (25 mM) medium with 10 nM of exendin-4, high-content time-lapse imaging was performed. *Supplementary Video S1* (Supplementary Data are available online at www.liebertpub.com/adt) shows real-time insulin vesicle movement in live cells during a glucose challenge. Overall, there was an outward mobilization of the reserve pool population toward the cell membrane that indicates increased insulin vesicle trafficking to replenish the RRP (*Supplementary Fig. S1*).

Assay Development to Identity Modulators of Insulin Granule Packaging

Parental INS-1 and the transfected INS-1 with PPI-mCherry were carried in parallel in all initial studies. The total fluorescent intensity in the red (675/50 nm) of parental INS-1 was similar to background wells with media alone. Bafilomycin is a vacuolar-type H^+ ATPase (V-ATPase) inhibitor that prevents insulin granule formation by inhibiting maturation of vacuoles.[20] To validate bafilomycin as a positive control for the HF-FP assay, optimization of bafilomycin concentration and incubation time were performed. The performance of FP assay was evaluated using Z′-factor and was calculated using the equation, where σ is standard deviation of positive control (maximum signal control; bafilomycin-treated) or negative

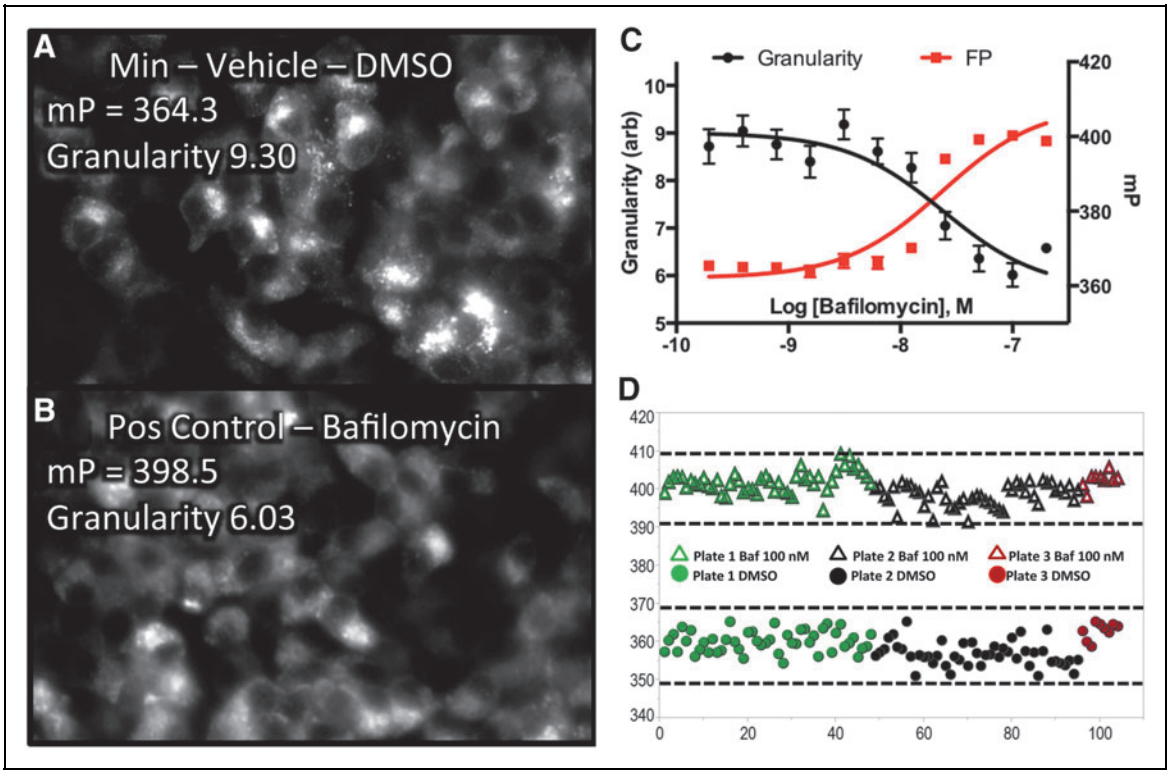

Fig. 5. Correlation between HF-FP signal and high-content endpoints and a Min–Max assay validation. **(A)** INS-1 PPI-mCherry vehicle control cells showing a granular insulin expression pattern. **(B)** 100 nM bafilomycin-treated cells showing a smooth expression pattern. **(C)** Partial least squares (PLSs) analysis revealed a strong anticorrelation between HF-FP signal and mCherry granularity. **(D)** Min–Max assay validation in 192 wells from three 96-well plates showing incubation with positive control (100 nM bafilomycin) and negative control (DMSO vehicle). The *dotted lines* indicate the range of $\mu \pm 3\sigma$ of positive and negative controls. The data are mean ± SE of four replicates.

control (minimum signal control; DMSO alone) and μ is the mean of the positive control or negative control:

$$Z' - \text{factor} = 1 - [3\sigma_{max} + 3\sigma_{min}]/[\mu_{max} - \mu_{min}].$$

Four-hour incubation with 100 nM bafilomycin resulted in maximum change in FP relative to negative control, providing the maximum assay window and the Z′-factor was greater than 0.5.

To aid in the interpretation of the FP phenomenon, PLS regression analysis was performed following high-content imaging. Cells were treated with 0.1–200 nM of bafilomycin and FP was measured using the PHERAstar plate reader. The plate was immediately fixed and stained with Hoechst-33342 and was imaged using a BD Pathway 855 BioImager. *Figure 5A* shows the negative control condition exhibiting a normal granular mCherry expression pattern. *Figure 5B* shows 100 nM bafilomycin-treated cells with a smooth mCherry expression pattern. PLSs regression analysis was performed at each bafilomycin concentration with high-content features as factors (X's), and were regressed against the FP value as the response variable (Y) to discover the high-content features most highly correlated with the FP signal. PLS analysis demonstrated high anticorrelation with the quantified granularity indicating that the HF-FP assay was primarily measuring the granularity of the PPI-mCherry signal (*Fig. 5C*). The calculated EC_{50} values of bafilomycin for FP and granularity were nearly identical at 23.3 and 24.0 nM, respectively.

To assess the day-to-day variability, a Min–Max experiment using 100 nM bafilomycin was performed on three different days (*Fig. 5D*). The coefficient of variation (CV) was 0.75% and 0.64% for Min control and Max control, respectively, and the 3-day variability was less than 5%. The calculated Z′-factor for each plate from three different days were 0.60 (plate 1, green), 0.57 (plate 2, black), and 0.68 (plate 3, red), respectively, indicating the suitability of the assay for HTS.

To examine the performance of the HF-FP assay in 384-well format, 20,000, 40,000, 60,000, and 80,000 cells/well seeding densities were assessed with 4 h incubation of 83 nM bafilomycin and 80,000 cells/well seeding density provided the maximum assay window in 384-well format. There were no significant differences in parallel and perpendicular intensities, and FP between 96- and 384-well plate formats. A Z′-factor over 0.5 was calculated for 384-well format when 80,000 cells/well seeding density and 83 nM bafilomycin were used (data not shown).

Pilot Screening in 384-Well Plate Format

We performed pilot screening using Prestwick and Enzo 384-well format for concentration range finding and to determine the confirmation rate. Plate-based normalization was performed using the mean polarization values of negative and positive controls, yielding percent inhibition from 0 to 100. The normalized FP is plotted for each compound in *Figure 6A* after omitting, for clarity, two hits that show 202.8% inhibition and −639.2% inhibition. Compounds were identified as hits if the mP values were above or below the 95% CL (approximately μ ± 3σ). The averaged Z′-factor from this 1,782 compound pilot screen was 0.52, with a hit rate of 1.4%. Twenty-six compounds were active. Antimycin A1 was selected from both FDA-approved and natural product libraries.

A histogram and box plot with a normal statistical distribution of compound activities are shown in *Figure 6B* and *C*. Eleven compounds out of the 26 selected compounds were screened in triplicate for dose–response determination and 4 were confirmed in this assay, yielding a confirmation rate of 36.4%. Antimycin A1, oligomycin A, and rotenone significantly decreased FP (*Fig. 7A–C*) and Chicago Sky Blue 6B significantly increased FP in a dose-dependent manner. However, Chicago Sky Blue 6B was considered a false positive due to fluorescence in the same spectral region as mCherry and it was not possible to separate its contribution to the overall FP signal. *Figure 7D* shows that antimycin A1

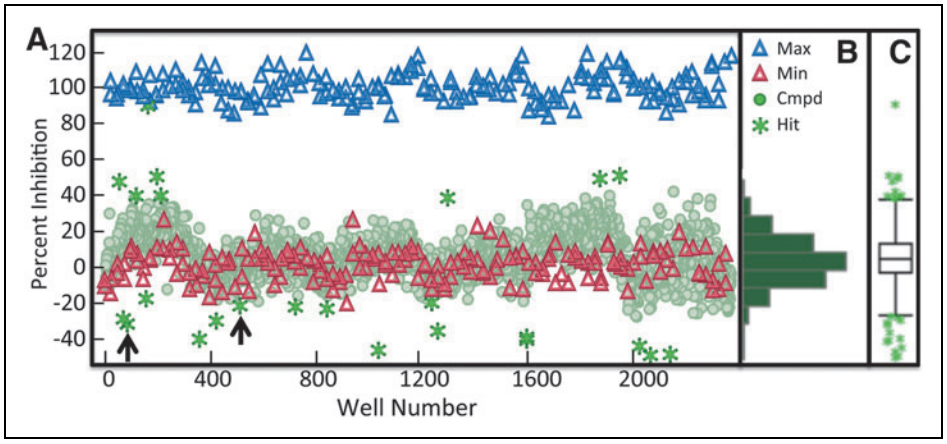

Fig. 6. FP data from pilot screen. **(A)** Scatterplot for 1,782 test compounds (*green circle*), negative control (DMSO; *red triangle*), and positive control (Bafilomycin; *blue triangle*). The *arrows* indicate antimycin A1 that were selected from both Prestwick and Enzo chemical libraries. **(B)** Histogram indicating normal statistical distribution of compounds (mean ± SD; 367.9 ± 7.3). **(C)** Box plot showing distribution statistics and outlier compounds.

© MARY ANN LIEBERT, INC.

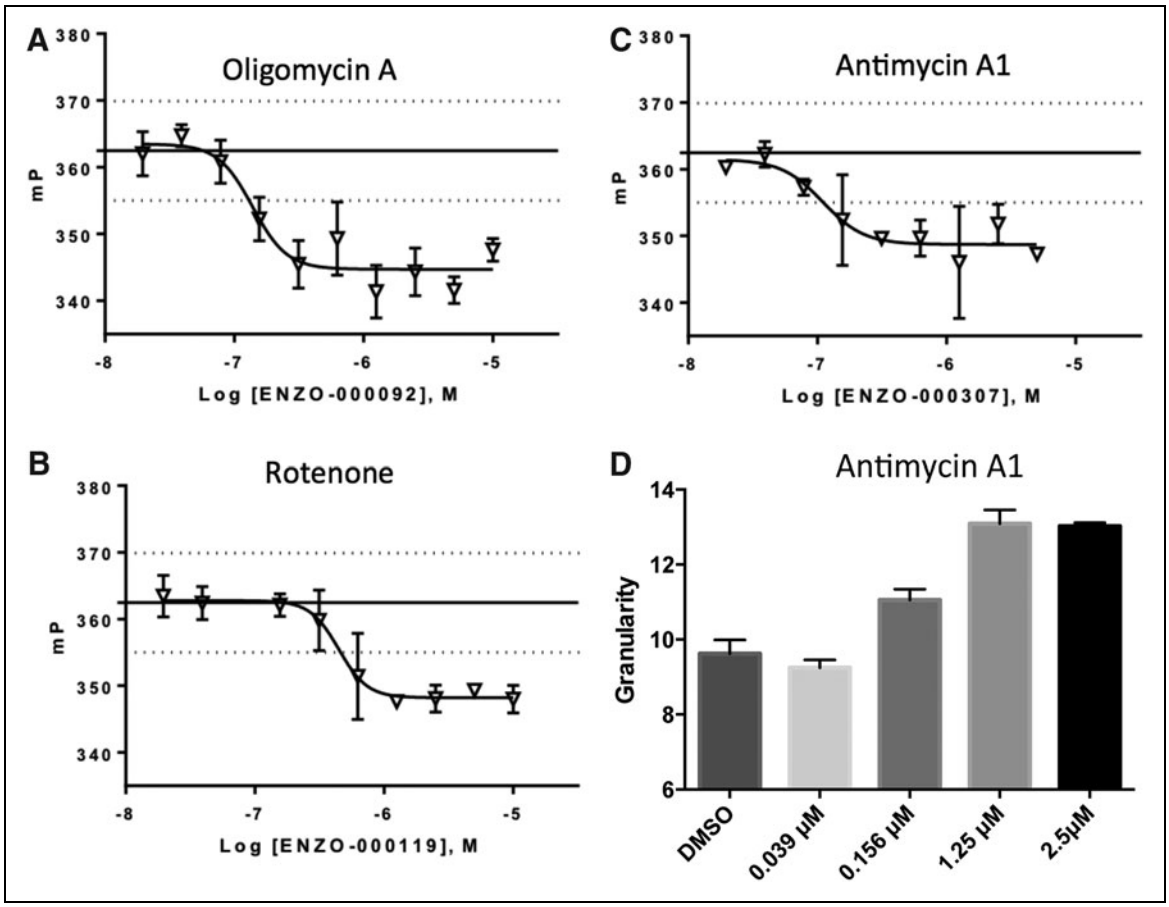

Fig. 7. Dose–response confirmation of active compounds that significantly decreased FP. **(A)** Oligomycin A, $EC_{50} = 0.114\ \mu M$. **(B)** Antimycin A1, $EC_{50} = 0.089\ \mu M$. **(C)** Rotenone, $EC_{50} = 0.37\ \mu M$. **(D)** Antimycin A1 increased granularity in a dose-dependent manner. *Dotted lines* depict the range of $\mu \pm 3\sigma$. Each value represents the mean ± SD of three replicates.

significantly increased granularity of PPI-mCherry signal in a dose-responsive manner, indicating that decrease in FP correlates with increase in insulin granularity, as shown in the PLS regression analysis.

DISCUSSION

Currently, there is a significant unmet medical need in the management of T2Ds. With only 36% of diabetes patients achieving their HbA1c goal of ≤7%, there is a dramatic need for new therapeutic approaches for the management of T2Ds.[9] One aspect of insulin production by the β-cell that has been elusive to drug discovery efforts is modulation of insulin granule packaging and trafficking. In this study, we present a high-throughput technique to assess insulin granule dynamics in cell lines that can be used to characterize pharmacological effects on granule formation and release. This technology provides a unique tool to assess an aspect of β-cell biology that has been inaccessible to HTS and can potentially lead to the discovery of small molecules that enhance insulin processing and delivery by the β-cell. This phenotypic drug discovery approach can also lead to the identification of novel molecular targets and new therapeutic strategies for the treatment of diabetes.

Utility and Benefits of PPI-mCherry Reporter System

In this study we present a genetically encoded mCherry-insulin reporter system that can be used in several ways, including live cell imaging of insulin and its dynamics, simple GSIS measurements, viable β-cell sorting, and live cell tracking of insulin granule dynamics with FP through homo-FRET interactions. This reporter system is generally responsive to known insulin modulating compounds and can be used as a surrogate signal in lieu of costly insulin immunolabeling approaches.

The current standard for detecting insulin secretion in GSIS is using insulin-ELISA. ELISA assays require expensive

reagents, including monoclonal antibodies and time-consuming assay optimization. Our reporter system allows the measurement of endpoint insulin secretion in a simpler way, by direct quantitation of media containing insulin-mCherry fusion protein using a fluorescence detector. Cell culture supernatant can simply be deposited onto a membrane and directly imaged using a TRITC filter set or in the 780 nm channel on an IR-based flat-bed scanner. While this technique is simple, it requires larger volumes of cell culture supernatant ($\sim$800 μL, and is most suitable to larger formats (*e.g.*, six-well dishes of cells).

Assay Development to Identify Regulators of Insulin Granule Packaging Using Homo-FRET Through Polarization

In an effort to develop a high-throughput assay to monitor insulin production, we initially attempted to use a mouse insulin promoter-driven PPI-mCherry construct with the hopes of detecting increases in insulin by monitoring mCherry fluorescence, but driven by a *bona fide* insulin promoter. Unfortunately, we did not observe significant differences in mCherry signal under glucose stimulation and chose instead to refocus the assay on insulin maturation, packaging, and distribution in the cell using high-content imaging. We also hypothesized that measuring FP of mCherry in live cells could yield information about insulin packaging. Indeed, a substantial difference in the FP signal was observed, but in the opposite direction, as predicted just considering the change in the tumbling rate of mCherry. Initial assumptions were that bafilomycin would cause a decrease in mCherry FP signal due to the increased tumbling rate of mCherry when not packaged into a granule. The observed effect was a large increase in the FP signal upon bafilomycin treatment, indicating an alternative mechanism. When insulin granules are tightly packaged in untreated control cells, the mCherry intermolecular distance decreases and homo-FRET increases. In this configuration, the excited state can hop from molecule to molecule, thereby randomizing the initial polarization information, which results in an apparent decrease of mCherry polarization. When PPI-mCherry-transfected cells receive bafilomycin, the insulin granule packaging and maturation process is inhibited and PPI-mCherry insulin fusion proteins are present mostly as monomers. Then, polarization of mCherry increases due to an inhibition of homo-FRET, caused by increased intermolecular distance of mCherry. Fluorescent images confirm that the PPI-mCherry-transfected cells were responsive to bafilomycin by demonstrating a diffuse pattern of mCherry, compared to untreated cells, which showed an intense punctate pattern of mCherry. Using bafilomycin as a positive control, we optimized the HF-FP assay to indicate the degree of insulin granule formation as measured by changes in FP of mCherry for both 96- and 384-well formats. We also successfully performed pilot screening in 384-well format.

Three compounds, antimycin A1, oligomycin A, and rotenone were discovered in the pilot screen and exhibited a dose-responsive decrease in FP. These compounds are mitochondrial toxins that inhibit the electron transport chain of oxidative phosphorylation at different stages.[21] Antimycin A1 inhibits electron transfer in complex-III by inhibiting the oxidation of ubiquinol by Cyt bc_1. Rotenone, an inhibitor of NADH dehydrogenase, and oligomycin A, an inhibitor of ATP synthase, inhibit the electron transfer in complex-I and V, respectively. In pancreatic β-cells, mitochondrial oxidative phosphorylation accounts for approximately 98% of ATP production.[22] Glucose is metabolized through mitochondrial oxidative phosphorylation and produces ATP. Numerous studies have demonstrated that antimycin A1, oligomycin A, and rotenone inhibit GSIS by interrupting mitochondrial oxidative phosphorylation.[21,23,24] The decreased ATP/ADP ratio by these mitochondrial toxins inhibits closure of ATP-sensitive K^+ channels, suppressing calcium influx and insulin secretion. In this assay, the shift in equilibrium to more tightly packaged mature insulin granules due to suppressed insulin secretion enhances homo-FRET and decreases FP. This phenomenon is verified by our result that insulin secretion inhibitors, antimycin A1, oligomycin A, and rotenone significantly decrease mCherry polarization. Additionally, in high-content imaging, an increase of antimycin A1 concentration significantly increased granularity in a dose-dependent manner indicating more tightly packaged mature insulin granules due to suppressed insulin secretion.

In conclusion, this insulin reporter system and HTS platform delivers a viable approach for phenotypic drug discovery for the identification of compounds that alter insulin granule packaging and insulin release and provides useful tools for live-cell imaging of insulin dynamics in β-cells. Additionally, we established a novel cell-based FP biosensor using a fluorescent PPI reporter to identify compounds that modulate insulin granule packaging. Several compounds were identified in this study that supported our assay mechanism, demonstrating that this assay tool is capable of a large-scale library screening. To expand on this study, the HF-FP approach needs to be evaluated for other fluorescent proteins and biological systems. This technology can provide a valuable new modality for HTS to assess protein–protein interactions and dynamics in live-cell systems.

ACKNOWLEDGMENTS

The research reported in this article was partially supported by the North Carolina Biotechnology Center Biotechnology

© MARY ANN LIEBERT, INC.

Research Grant (BRG) program grant number BRG-1212 to J.Z.S. The authors would also like to thank Mark Rizzo for thoughtful discussions on fluorescent protein-related phenomena.

DISCLOSURE STATEMENT

No competing financial interests exist.

REFERENCES

1. Rorsman P, Eliasson L, Renstrom E, Gromada J, Barg S, Gopel S: The cell physiology of biphasic insulin secretion. *News Physiol Sci* 2000;15:72–77.
2. (CDC) CfDCaP: 2014 National Diabetes Statistics Report. 2014.
3. Huang CJ, Lin CY, Haataja L, *et al.*: High expression rates of human islet amyloid polypeptide induce endoplasmic reticulum stress mediated beta-cell apoptosis, a characteristic of humans with type 2 but not type 1 diabetes. *Diabetes* 2007;56:2016–2027.
4. (CDC) CfDCaP: 2007 National Diabetes Fact Sheet. 2007.
5. Association AD: Standards of medical care in diabetes—2010. *Diabetes Care* 2010;33:S4, S4–S10.
6. Nauck MA: Unraveling the science of incretin biology. *Am J Med* 2009;122:S3–S10.
7. Del Prato S, Penno G, Miccoli R: Changing the treatment paradigm for type 2 diabetes. *Diabetes Care* 2009;32 Suppl 2:S217–S222.
8. Cefalu WT: The physiologic role of incretin hormones: clinical applications. *J Am Osteopath Assoc* 2010;110:S8–S14.
9. Meece J: Dispelling myths and removing barriers about insulin in type 2 diabetes. *Diabetes Educ* 2006;32:9S–18S.
10. Kim W, Egan JM: The role of incretins in glucose homeostasis and diabetes treatment. *Pharmacol Rev* 2008;60:470–512.
11. Hao M, Li X, Rizzo MA, Rocheleau JV, Dawant BM, Piston DW: Regulation of two insulin granule populations within the reserve pool by distinct calcium sources. *J Cell Sci* 2005;118:5873–5884.
12. Chan FT, Kaminski CF, Kaminski Schierle GS: HomoFRET fluorescence anisotropy imaging as a tool to study molecular self-assembly in live cells. *Chemphyschem* 2011;12:500–509.
13. Tramier M, Coppey-Moisan M: Fluorescence anisotropy imaging microscopy for homo-FRET in living cells. *Methods Cell Biol* 2008;85:395–414.
14. Bader AN, Hofman EG, Voortman J, en Henegouwen PM, Gerritsen HC: Homo-FRET imaging enables quantification of protein cluster sizes with subcellular resolution. *Biophys J* 2009;97:2613–2622.
15. Watkins S, Geng X, Li L, Papworth G, Robbins PD, Drain P: Imaging secretory vesicles by fluorescent protein insertion in propeptide rather than mature secreted peptide. *Traffic* 2002;3:461–471.
16. Tillmar L, Carlsson C, Welsh N: Control of insulin mRNA stability in rat pancreatic islets. Regulatory role of a 3′-untranslated region pyrimidine-rich sequence. *J Biol Chem* 2002;277:1099–1106.
17. Tillmar L, Welsh N: Glucose-induced binding of the polypyrimidine tract-binding protein (PTB) to the 3′-untranslated region of the insulin mRNA (ins-PRS) is inhibited by rapamycin. *Mol Cell Biochem* 2004;260:85–90.
18. Carpenter AE, Jones TR, Lamprecht MR, *et al.*: CellProfiler: image analysis software for identifying and quantifying cell phenotypes. *Genome Biol* 2006;7:R100.
19. Larsson-Nyren G, Sehlin J: Interaction between perchlorate and nifedipine on insulin secretion from mouse pancreatic islets. *Biosci Rep*1993;13:107–117.
20. Sun-Wada GH, Toyomura T, Murata Y, Yamamoto A, Futai M, Wada Y: The a3 isoform of V-ATPase regulates insulin secretion from pancreatic beta-cells. *J Cell Sci* 2006;119:4531–4540.
21. Alarcon C, Wicksteed B, Prentki M, Corkey BE, Rhodes CJ: Succinate is a preferential metabolic stimulus-coupling signal for glucose-induced proinsulin biosynthesis translation. *Diabetes* 2002;51:2496–2504.
22. Erecinska M, Bryla J, Michalik M, Meglasson MD, Nelson D: Energy metabolism in islets of Langerhans. *Biochim Biophys Acta* 1992;1101:273–295.
23. Kiranadi B, Bangham JA, Smith PA: Inhibition of electrical activity in mouse pancreatic beta-cells by the ATP/ADP translocase inhibitor, bongkrekic acid. *FEBS Lett* 1991;283:93–96.
24. Mertz RJ, Worley JF, Spencer B, Johnson JH, Dukes ID: Activation of stimulus-secretion coupling in pancreatic beta-cells by specific products of glucose metabolism. Evidence for privileged signaling by glycolysis. *J Biol Chem* 1996;271:4838–4845.

Address correspondence to:
Jonathan Z. Sexton, PhD
Biomanufacturing Research Institute and Technology Enterprise
Department of Pharmaceutical Sciences
North Carolina Central University
Durham, NC 27707

E-mail: jsexton@nccu.edu

Abbreviations Used

BSA = bovine serum albumin
CMV = cytomegalovirus
DMEM = Dulbecco's modified Eagle's medium
DMSO = dimethyl sulfoxide
FBS = fetal bovine serum
FP = fluorescence polarization
FRET = Förster resonance energy transfer
GFP = green fluorescent protein
GLP-1 = glucagon-like peptide-1
GLP-1R = glucagon-like peptide-1 receptor
GSIS = glucose-stimulated insulin secretion
HTS = high-throughput screening
INS-1 = rat insulinoma cells
PBS = phosphate-buffered saline
PLS = partial least squares
PPI = preproinsulin
RRP = readily releasable pool
T2D = type 2 diabetes